

# A quantum chemical study of tertiary carbenium ions in acid catalyzed hydrocarbon conversions over phosphotungstic acid

Michael J. Janik, Robert J. Davis, Matthew Neurock\*

*University of Virginia, 102 Engineers' Way, Charlottesville, VA 22904, United States*

Available online 15 May 2006

## Abstract

The formation and transformation of adsorbed alkoxide intermediates to active carbenium-ion species over solid acid catalysts are essential steps that determine the rate and selectivity of many hydrocarbon conversion processes. Herein, density functional theory is used to examine these processes for a *t*-butyl species adsorbed to phosphotungstic acid, a Keggin structured polyoxometalate. The tertiary carbenium ion is found to be a meta-stable intermediate state. The conversion of a physisorbed,  $\pi$ -bound isobutene state to the *t*-butyl alkoxide state occurs in a two-step process through formation of this tertiary carbenium-ion intermediate. Both the intermediate and transition states contain a positive charge and are properly termed carbenium ions, and the interaction with the catalyst surface is mainly Coulombic. The dehydrogenation of isobutane and the dehydration of 2-methyl-2-propanol are also examined. Tertiary carbenium ions are found to be transition states for both of these processes as well.

© 2006 Elsevier B.V. All rights reserved.

**Keywords:** Heteropolyacid; Phosphotungstic acid; Solid acid; Alkene adsorption; Alkane protolysis; Alcohol dehydration; DFT; Carbenium ion

## 1. Introduction

The mechanism for transformation of hydrocarbons over solid acids involves the formation and conversion of adsorbed carbocations as active intermediates. The lowest energy equilibrium state for a small alkyl fragment adsorbed on a solid acid is typically an alkoxide, in which a covalent bond is formed between a carbon atom of the alkyl group and an oxygen atom of the acid's conjugate base [1,2]. Contrarily, the equilibrium state of an alkyl species in a highly concentrated liquid superacid is a solvated carbenium ion [3,4]. Liquid and solid acid catalysts show similar product distributions for a reaction such as the alkylation of isobutane with butene [5], leading to speculation that the "active species" for hydrocarbon transformations over solid acids is also a carbenium ion [6]. Characterization of the interaction of the adsorbed alkyl species on the solid acid and of the transformation between the alkoxide and carbenium-ion states is essential to understanding the factors that influence hydrocarbon conversion processes. Herein, we report that over phosphotungstic heteropolyacid, a carbenium ion is both a transition state and a meta-stable

intermediate state for conversion from the adsorbed alkoxide equilibrium state.

Phosphotungstic acid ( $\text{H}_3\text{PW}_{12}\text{O}_{40}$ , HPW) is one in a class of materials known as heteropolyacids (HPAs) or polyoxometalates. The well-defined molecular structure of HPW is known as a Keggin unit, in which a central  $\text{PO}_4$  tetrahedron is surrounded by a  $\text{W}_{12}\text{O}_{36}$  shell, as shown in Fig. 1. A formal  $-3$  charge is imparted to the structure by the central tetrahedron, which is countered by acidic protons bound to the exterior oxygen atoms. There are three types of oxygen atoms at the exterior of the structure: terminal oxygen atoms ( $\text{O}_\text{t}$ ), which bind to a single tungsten atom; and two types of bridging oxygen atoms ( $\text{O}_\text{b}$  and  $\text{O}_\text{c}$ ), which link tungsten atoms, as indicated in Fig. 1. Keggin structured HPAs can be formed with various central or addenda atoms [7,8]. The combination of a phosphorus central atom and tungsten addenda atoms has been shown to produce the strongest acid [8–10].

We have previously published a comparison between calculated and experimental adsorption energies of alkenes to HPAs [11]. Adsorption is initiated by the formation of a  $\pi$ -bound state, as is illustrated in Scheme 1 for an isobutene adsorbate. In the  $\pi$ -bound state, the alkene interacts by donating electron density from the C–C double bond to the HPA proton. The adsorption energy of alkene in a  $\pi$ -bound state is similar ( $\sim 40 \text{ kJ mol}^{-1}$ ) regardless of which alkene (primary,

\* Corresponding author. Tel.: +1 434 924 6248; fax: +1 434 982 2658.

E-mail address: [mn4n@virginia.edu](mailto:mn4n@virginia.edu) (M. Neurock).

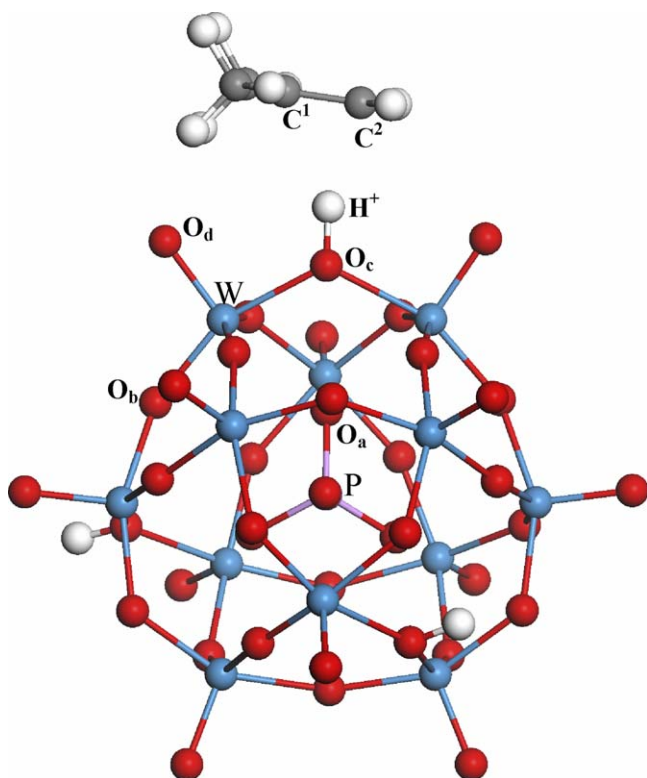


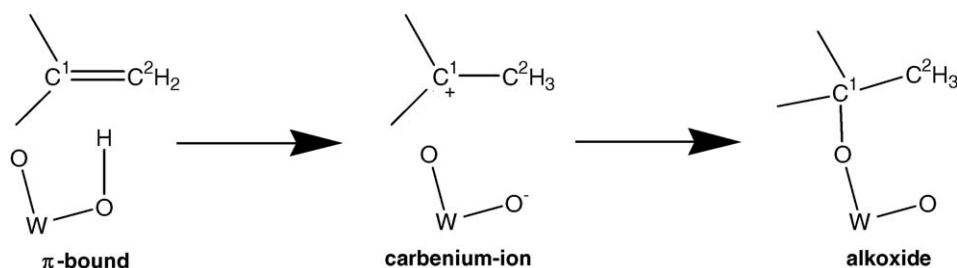
Fig. 1. The  $\pi$ -bound state of a *t*-butyl species on phosphotungstic acid.

secondary, or tertiary) is adsorbed. Donation of the proton to one side of the double bond ( $C^2$  in Scheme 1) produces a carbenium ion, with a formal positive charge on the opposite carbon of the double bond ( $C^1$ ). A covalent bond is then formed between the unsaturated carbon atom ( $C^1$ ) and an oxygen atom of the conjugate base of the solid acid, forming the alkoxide state. The carbenium-ion state formed on solid acids is typically described as a transition state between the  $\pi$ -bound and alkoxide states [12–18]. The activation energy to form the carbenium-ion from the  $\pi$ -bound alkene is lower for a more substituted  $C^1$  atom (i.e. tertiary < secondary < primary). This same adsorption process and relative trend are reported for alkene adsorption over zeolites [12–18]. The calculated adsorption energies, however, are more exothermic and the activation barriers are lower over HPW than those observed in the zeolite. In the case of an iso-alkyl species, however, the potential energy surface along the transformation is rather flat (i.e. the potential energy changes relatively little with respect to the reaction coordinate) and a detailed

characterization of the carbenium-ion state has not been previously reported.

Previous computational studies have indicated that the lowest energy state for an adsorbed alkyl species is the alkoxide [12–15]. However, for the *t*-butyl species, the carbenium ion state is only slightly higher in energy. A few theoretical studies have illustrated that the enhanced stability of the tertiary carbenium ion leads to differences in its surface behavior. Rozanska et al. found that the alkoxide is only slightly lower in energy compared to the tertiary carbenium ion, and that, due to steric interactions between the alkoxide and smaller pore zeolite structures, the  $\pi$ -complex may be favored [16]. A recent study by Corma and co-workers [19] reports that a meta-stable *t*-butyl carbenium-ion intermediate exists in mordenite, and that the  $\pi$ -complex is actually the lowest energy adsorbed state of isobutene. Sinclair et al. noted that the carbenium ion may represent a short-lived intermediate in certain zeolite structures [13]. Molecular dynamics simulations indicate that the carbenium ion may desorb intact at high temperatures over gmelinite [20]. The greater stability of the tertiary carbenium ion leads to a weaker interaction with the catalyst surface than the less substituted carbenium ions, and therefore more closely represents a free carbocationic intermediate [13,16]. The potential energy surface for the displacement of the tertiary carbenium ion is very flat, thus making the location of saddle points using quantum-chemical methods challenging [21].

The transformation between the alkoxide and carbenium-ion states is a key step in many hydrocarbon conversion processes. Aside from the formation of alkoxides from alkene adsorption, alkoxide intermediates also occur in alkane and alcohol transformations over solid acids [22,23]. Although the alkoxide has been identified as the minimum energy adsorbed state of an alkyl species over a solid acid [1,2], the relative stability of a carbenium-ion state is invoked to explain the product distribution for hydrocarbon transformations. For example, the alkylation of isobutane with butenes forms predominantly isoalkane products, indicating that hydride transfer (the transfer of  $H^-$  from an alkane to the adsorbed alkyl species) is faster to a tertiary carbon atom [24]. Theoretical studies of hydrocarbon conversions over zeolites have concluded that carbenium ions represent the transition states for many hydrocarbon conversions, including alkene adsorption [12–18], alkene double bond shift [25], alkane protolysis/dehydrogenation [18,26–28], structural isomerization [21,29], cracking or oligomerization [18,21,28],  $\beta$ -scission or alkylation [21,30], and hydride transfer [21,25]. As the stability of carbenium ions controls



Scheme 1. The mechanism of alkene adsorption over phosphotungstic acid. The tungsten-oxygen fragment represents a section of the Keggin unit.

the activity and selectivity for many hydrocarbon conversion processes, the detailed understanding of their formation and interaction with the catalyst surface is necessary to fully understand the potential of these processes and to aid in the design of new solid acids.

In this work, we illustrate that a tertiary carbenium ion is a meta-stable intermediate along the reaction path for conversion between the  $\pi$ -bound state and the alkoxide state of an adsorbed *t*-butyl species over phosphotungstic acid. Detailed characterization of the reaction path is reported, in which transition states are located for conversion between the meta-stable carbenium ion and the two equilibrium adsorbed states. Finally, tertiary carbenium ions are also identified as transition states for the protolytic activation of isobutane and the dehydration of 2-methyl-2-propanol.

## 2. Computational methods

Ab initio quantum-chemical calculations were carried out using plane-wave gradient-corrected density functional theory as implemented in the Vienna ab initio Simulation Package (VASP) [31–33]. Ultrasoft pseudopotentials were used to describe electron-ion interactions [34]. The Perdew-Wang (PW91) form of the generalized gradient approximation was used to calculate the exchange and correlation energies [35]. A cutoff energy of 396.0 eV for the plane-wave basis set was employed in all calculations. The single Keggin unit molecular system was represented within the periodic code by using a  $20 \text{ \AA} \times 20 \text{ \AA} \times 20 \text{ \AA}$  unit cell. The convergence was confirmed with respect to cell size for both equilibrium and transition states. The Brillouin zone sampling was restricted to the  $\Gamma$ -point. This method has previously been shown to determine an equilibrium Keggin structure in reliable agreement with experiment [36].

The nudged elastic band method was used within VASP to isolate transition states [37,38]. The climbing image method (NEB-CI) was employed, in which the highest energy image is required to climb up in energy along the elastic band to better estimate the saddle point along the minimum energy reaction path [39]. Four images between the initial and final states were used in each search. A transition state was identified as the image with a maximum in energy and an absolute tangential force less than  $0.04 \text{ eV \AA}^{-1}$ . This image was subsequently relaxed until the forces on each atom were less than  $0.06 \text{ eV \AA}^{-1}$ .

The harmonic vibrational modes were calculated to confirm equilibrium and transition states as well as to determine zero-point vibrational energy (ZPVE) corrections to the total energies. Positive and negative displacements of  $0.01 \text{ \AA}$  in each of the Cartesian coordinates were used to determine the Hessian matrix. The calculation of second derivatives using finite differences for all of the modes of the Keggin structure was computationally prohibitive. Constrained vibrational calculations were carried out instead, in which the Hessian matrix is determined for a subset of relevant atoms in the Keggin structure. The ZPVE corrections reported are approximated by including only vibrational modes associated with the adsorbate

and the binding area of the Keggin unit (two adjacent W atoms, four bridging oxygen atoms, and two terminal oxygen atoms). In some cases, imaginary vibrational frequencies were determined for rotation of methyl groups in optimized (equilibrium and transition state) structures. In these cases, the atoms were displaced slightly along the imaginary vibrational mode and re-optimized until the inappropriate imaginary frequencies were removed. This “manual optimization” of methyl rotations did not change the total energy by more than a few  $\text{kJ mol}^{-1}$ .

Atomic charges of the alkyl species were determined using site projected atomic charge densities, with a Wigner Seitz radius of 1.05 for carbon and 0.76 for hydrogen. These values were chosen because they provide a correct count of the total number of valence electrons in gas-phase isobutene (24.02) and isobutane (25.98) molecules. However, the total valence electrons on the gas-phase *t*-butyl cation is counted as 24.69 rather than the correct value of 24.00.

## 3. Results and discussion

### 3.1. Adsorbed *t*-butyl transformation

Prior to examining the reaction coordinate for *t*-butyl transformation, the preferred sites for the alkoxide and  $\pi$ -bound species must be identified. The *t*-butyl alkoxide preferentially forms on a terminal oxygen atom of the Keggin unit. The terminal alkoxide (i.e. a *t*-butyl group bound to  $\text{O}_d$  in Fig. 1) is  $76.4 \text{ kJ mol}^{-1}$  more stable than a bridging alkoxide (*t*-butyl group bound to  $\text{O}_b$ ). This preference may be due to repulsion that arises in the bridging position due to interactions of the methyl groups of the adsorbate and oxygen atoms at the exterior of the Keggin unit, though differences in the chemical bonding with the different types of oxygen atoms cannot be excluded. The  $\pi$ -bound species shows little preference for proton location, as the alkyl fragment is further from the Keggin unit. Adsorption of the  $\pi$ -bound state at an  $\text{H-O}_c$  site is  $11.9 \text{ kJ mol}^{-1}$  more stable than adsorption at an  $\text{H-O}_d$  site, which is approximately the same as the energetic preference for a proton to locate at the  $\text{O}_c$  atom [36]. Fig. 1 illustrates a  $\pi$ -bound isobutene molecule on the  $\text{H-O}_c$  bridge site. The tertiary carbon atom is labeled  $\text{C}^1$  and the other carbon atom of the double bond is labeled  $\text{C}^2$ . Bhan et al. [14] found that, for adsorption of propene to H-ZSM-5 zeolite, the activation barrier for alkoxide formation at the same oxygen atom on which the proton was initially bound is  $20.1 \text{ kJ mol}^{-1}$  higher in energy than the barrier that results from alkoxide formation via a dual-site mechanism. We only consider a dual-site mechanism for *t*-butyl transformation, with the  $\pi$ -bound state interacting with a proton on an  $\text{O}_c$  atom and the alkoxide forming on an  $\text{O}_d$  atom.

Fig. 2 illustrates the reaction energy diagram for transformation of the adsorbed olefin from the  $\pi$ -bound state to the alkoxide state, whereas Table 1 details the interatomic distances within the extrema along the reaction coordinate. Both the  $\pi$ -bound (A in Fig. 2) and alkoxide (E) states were confirmed to have all real vibrational frequencies. The  $\pi$ -bound state was

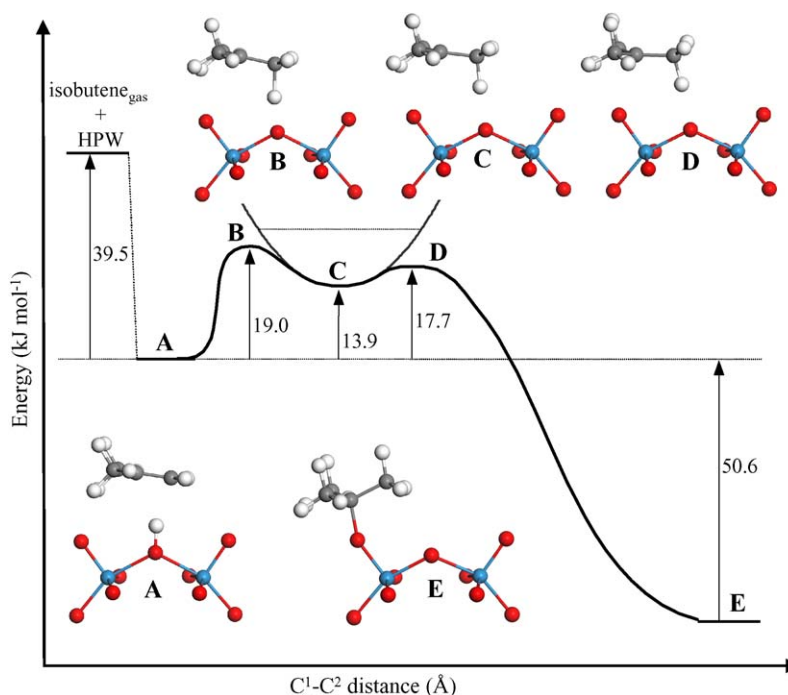


Fig. 2. Reaction energy diagram for transformation of an adsorbed *t*-butyl group over phosphotungstic acid. Interatomic distances within these structures are given in Table 1. The harmonic oscillator approximated energy well is sketched for state C to illustrate that the harmonic ground vibrational state is higher in energy than the transition states (B and D). Only a portion of the Keggin unit is shown, however, all calculations were performed with the entire Keggin unit.

calculated to be  $39.5 \text{ kJ mol}^{-1}$  more stable than separated isobutene and phosphotungstic acid species. The alkoxide state was found to be  $50.6 \text{ kJ mol}^{-1}$  more stable than the  $\pi$ -bound state. A single NEB-CI transition state search between the  $\pi$ -bound and alkoxide states located a transition state similar in structure and energy to **D** in Fig. 2. This structure has a single imaginary frequency;  $88i \text{ cm}^{-1}$ , however, displacement along this mode towards the  $\pi$ -bound state and subsequent optimization yields structure **C**, a meta-stable carbenium-ion intermediate. Structure **C** has all real frequencies, confirming it represents a minimum along the reaction coordinate. This carbenium-ion state is  $13.9 \text{ kJ mol}^{-1}$  less stable than the  $\pi$ -bound state (**A**) and  $64.5 \text{ kJ mol}^{-1}$  less stable than the alkoxide (**E**). In this carbenium-ion structure, proton donation from the HPA is essentially complete, with a  $\text{C}^2\text{--H}$  distance of  $1.17 \text{ \AA}$ . The hybridization of the  $\text{C}^2$  atom is converted from  $\text{sp}^2$  to  $\text{sp}^3$ , while the  $\text{C}^1$  atom remains  $\text{sp}^2$  hybridized and in the same plane as its substituents. The  $\text{C}^1\text{--C}^2$  distance lengthens from  $1.35 \text{ \AA}$  in

**A** to  $1.43 \text{ \AA}$  in **C**, similar to the DFT calculated  $\text{C--C}$  distance of  $1.46 \text{ \AA}$  in a gas-phase *t*-butyl carbenium ion.

Two NEB-CI searches were conducted to locate transition states between the two stable adsorbed species and the carbenium-ion intermediate. The transition state between the  $\pi$ -bound (**A**) and carbenium-ion (**C**) states is labeled **B**, and is formed with an activation barrier of  $19.0 \text{ kJ mol}^{-1}$  from the  $\pi$ -bound state. Structure **B** has a single imaginary frequency of  $639i \text{ cm}^{-1}$ , confirming it is a transition state. The reactive mode involves proton donation from the HPA to  $\text{C}^2$  with lengthening of the  $\text{C}^1\text{--C}^2$  bond. However, there is no indication of alkoxide formation in this reactive mode, as there is no movement of the  $\text{O}_d$  atom.

The transition state between the meta-stable carbenium ion (**C**) and the alkoxide (**E**) is labeled **D**, and is  $17.7 \text{ kJ mol}^{-1}$  higher in energy than the  $\pi$ -bound state. Structure **D** has a single imaginary frequency of  $82i \text{ cm}^{-1}$  confirming that it is a transition state. The low imaginary frequency indicates that

Table 1

The relative energies, imaginary frequencies, and interatomic distances of the equilibrium and transition states for a *t*-butyl species adsorbed to phosphotungstic acid

State <sup>a</sup>	RE <sup>b</sup> (kJ mol <sup>-1</sup> )	RE ZPVE <sup>c</sup> (kJ mol <sup>-1</sup> )	Imag freq. (cm <sup>-1</sup> )	$\text{O}_c\text{--H}^+$ (Å)	$\text{H}^+\text{--C}^2$ (Å)	$\text{C}^1\text{--C}^2$ (Å)	$\text{C}^1\text{--O}_d$ (Å)	$\text{W--O}_d$ (Å)
A	0.0	0.0	None	1.02	1.91	1.35	3.36	1.71
B	19.0	4.2	$639i$	1.37	1.29	1.39	2.86	1.72
C	13.9	10.1	None	1.67	1.17	1.43	2.68	1.73
D	17.7	10.3	$82i$	1.76	1.14	1.44	2.38	1.74
E	-50.6	-49.6	None	2.80	1.10	1.52	1.50	1.81

<sup>a</sup> The states for adsorption are illustrated in Fig. 2, and discussed in the text.

<sup>b</sup> The adsorption energy of State A ( $\pi$ -bound) relative to separated isobutene and phosphotungstic acid is  $-39.5 \text{ kJ mol}^{-1}$ .

<sup>c</sup> Please see the text for a discussion on the accuracy of ZPVE corrections using harmonic frequencies in this case. The ZPVE corrected adsorption energy of State A is  $-25.9 \text{ kJ mol}^{-1}$ .

alkoxide formation occurs over a flat barrier. The active mode for alkoxide formation involves a shifting of the carbenium ion to align the unsaturated carbon atom with the lone-pair of the  $O_d$  atom, along with a slight lengthening of the  $W-O_d$  bond. All equilibrium and transition states along the reaction path are more stable than the separated HPW and isobutene fragments. Structure **D** is equivalent within the convergence criterion employed to the transition state located in the full search from the  $\pi$ -bound state to the alkoxide, and is similar to the single transition state typically reported for alkene adsorption, in which proton donation is complete. The proton-donation transition state (**B**) was not located using a single NEB search between the  $\pi$ -bound state and the alkoxide, as the method examines only a finite number of points along the reaction coordinate and the proton donation step occurs over a steeper reaction barrier. The fragmented search, using the climbing NEB method, was necessary to locate this transition state.

The results of a charge analysis on the alkyl fragments of Fig. 2 are presented in Table 2. In the  $\pi$ -bound state (**A**), the *t*-butyl fragment retains the same number of valence electrons as the gas-phase isobutene molecule. The charge analysis indicates that the meta-stable carbenium-ion (**C**) and the transition states (**B**, **D**, and **D'**) have similar charges to a gas-phase carbenium ion. As all these structures are within  $5.1 \text{ kJ mol}^{-1}$  in energy; the potential energy surface along the *t*-butyl transformation coordinate is extremely flat, with both transition states and intermediate properly referred to as carbenium ions. In the alkoxide (**E**), the charge analysis is consistent with a neutral adsorbate forming a non-polar covalent bond.

Zero-point vibrational energy corrections reduce the energy of the carbenium-ion states with respect to the equilibrium states due to the loss of a vibrational degree of freedom at the transition state. However, the small energy differences between the intermediate and transition states and the flat potential energy surface lead to inaccuracies in making the harmonic oscillator approximation. The calculated ZPVE corrections here lead to the intermediate carbenium ion (**C**) being less stable than transition state **B** and only slightly more stable than transition state **D**. As illustrated in Fig. 2, the zeroth harmonic vibrational state is predicted to be a higher energy than the

calculated potential energy surface, indicating that the harmonic approximation does not hold for the flat PES of this reaction. However, independent of the method used to calculate the frequencies, the loss of a vibrational degree of freedom at the transition state will certainly lead to a lowering of the ZPVE-corrected total energy of the transition state compared to equilibrium states. Therefore, the maximum difference in energy between the transition states (**B**, **D**) and the carbenium-ion intermediate state is the non-corrected value of  $5.1 \text{ kJ mol}^{-1}$ , and the overall activation barrier for the conversion from the  $\pi$ -bound state to the alkoxide state is approximately  $10\text{--}15 \text{ kJ mol}^{-1}$ . The small energy differences between the intermediate and transition states indicate that, within a classical transition state theory approach to rate determination, the complex shape of the PES will have little effect on the overall rate of conversion between adsorbed states. The use of more complex rate theories or ab initio molecular dynamics would be necessary to determine if the complex shape of this reaction coordinate affects the rate of hydrocarbon conversion.

The transformation of the *t*-butyl species can be compared to conversion of *s*-butyl, which involves formation of a secondary carbenium ion. For *trans*-2-butene, the adsorption energy to the  $\pi$ -bound state is  $-30.8 \text{ kJ mol}^{-1}$ . The adsorption to form the alkoxide is  $38.4 \text{ kJ mol}^{-1}$  more stable than that to form the  $\pi$ -bound state. A single transition state, illustrated in Fig. 3, is located between the  $\pi$ -bound state and the alkoxide, with an

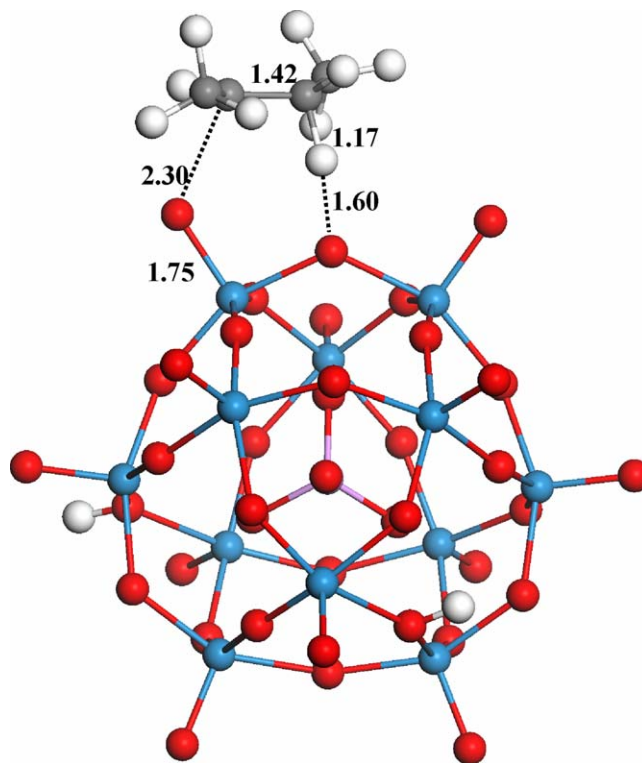


Fig. 3. The secondary carbenium-ion transition state for adsorption of *trans*-2-butene. The activation barrier from the  $\pi$ -bound state (not shown) is  $46.3 \text{ kJ mol}^{-1}$ , and the transition state has a single imaginary frequency of  $262i \text{ cm}^{-1}$ . Distances are in Å.

Table 2

Number of valence electrons in the *t*-butyl species adsorbed to phosphotungstic acid at each of the equilibrium and transition states illustrated in Fig. 2.

State	No. of valence electrons
Gas-phase isobutene	24.02
Gas-phase <i>t</i> -butyl cation	24.69
Gas-phase isobutene	25.98
<b>A</b> <sup>a</sup>	24.01
<b>B</b> <sup>a</sup>	23.96
<b>B</b> <sup>b</sup>	24.76
<b>C</b> <sup>b</sup>	24.76
<b>D</b> <sup>b</sup>	24.79
<b>E</b> <sup>b</sup>	24.96

<sup>a</sup> Electron count does not include those assigned to proton with which the *t*-butyl group is interacting.

<sup>b</sup> Electron count includes the proton donated from HPW to isobutene.

activation barrier of  $46.3 \text{ kJ mol}^{-1}$  determined with respect to the  $\pi$ -bound state and a single imaginary frequency of  $262i \text{ cm}^{-1}$ . The greater activation barrier ( $46.3$  for *s*-butyl versus  $19.0$  for *t*-butyl) is expected for the secondary carbenium ion. Displacement of the carbenium-ion atoms along the imaginary frequency vector in either direction, followed by structural optimization, converges to the two distinct equilibrium states. This indicates that there is a single transition state for the conversion of the *s*-butyl species between the  $\pi$ -bound state and the alkoxide, as the method which was used to locate the stable tertiary carbenium-ion intermediate did not find a stable intermediate for the secondary ion. The *s*-butyl carbenium ion is higher in energy than the separated *trans*-2-butene and HPW species, in contrast with the more stable tertiary carbenium ion. The higher activation barrier for formation of a secondary carbenium ion is typically invoked to explain why hydrocarbon conversion processes involving tertiary carbon atoms occur at higher rates.

### 3.2. Interaction of the carbenium ion with HPW

Fig. 4 illustrates an iso-density surface showing the electron distribution of the meta-stable *t*-butyl carbenium-ion state (C). There is little electron density overlap between the  $\text{O}_d$  atom and the tertiary carbon compared to the electron overlap observed in bonding regions between atoms, further indicating the free nature of the carbenium ion. However, the electron density plot does show an interaction between the  $\text{O}_c$  atom of HPW and the proton that has been donated. To analyze the

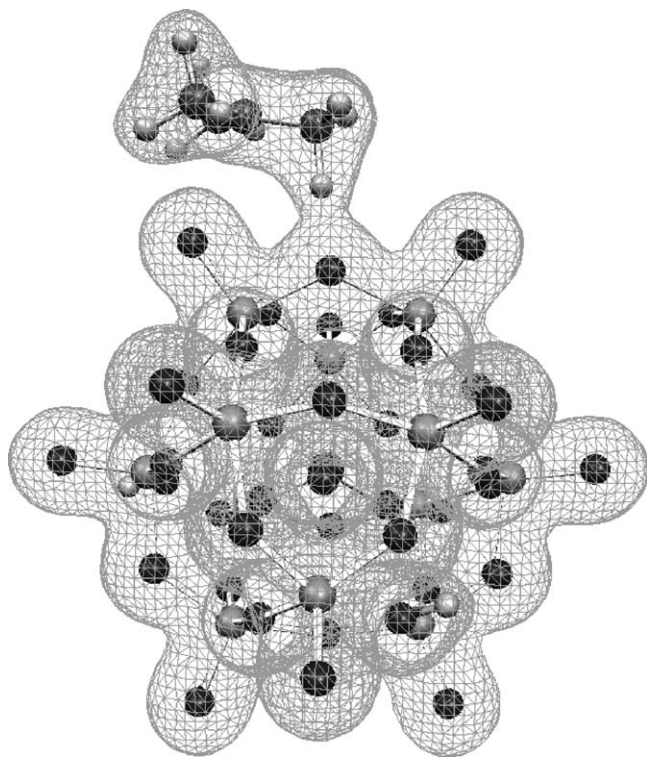


Fig. 4. An iso-density surface plot of the electron distribution of the meta-stable tertiary carbenium ion over HPW (C in Fig. 1). This surface encloses 97.1% of the total electron density.

interaction of the carbenium ion with the catalyst surface, it is helpful to define the zwitterion interaction energy,  $E_{\text{int}}$ , as

$$E_{\text{int}} = E_{\text{tbutyl-HPW}} - E_{\text{tbutyl}} - E_{\text{HPW-}} \quad (1)$$

where  $E_{\text{tbutyl-HPW}}$  represents the energy of the combined adsorbate–catalyst system for which  $E_{\text{int}}$  is evaluated,  $E_{\text{tbutyl}}$  represents the energy of a gas-phase *t*-butyl carbenium ion, and  $E_{\text{HPW-}}$  represents the energy of the conjugate base of HPW. The interaction energy of the carbenium ion with the HPW anion in structure C is  $-251.5 \text{ kJ mol}^{-1}$ , indicating that over  $250 \text{ kJ mol}^{-1}$  of energy would be needed in order to separate the positively-charged carbenium ion from the negatively charged catalyst surface.

The distance between the Keggin unit and the carbenium ion was displaced in a series of single-point calculations to understand the dependence of the interaction energy on the location of the carbenium ion. The carbenium ion was displaced in increments of  $0.1 \text{ \AA}$  along the vector connecting the central P and the  $\text{O}_c$  atoms (labeled in Fig. 1). Displacement in both the positive and negative directions was endothermic, confirming that structure C represents an optimum along this vector.

The interaction energy,  $E_{\text{int}}$ , is plotted as a function of distance from the equilibrium position ( $\Delta r$ ) in Fig. 5. At the furthest displacement (chosen to be  $1.3 \text{ \AA}$ ), the interaction can be approximated as purely Coulombic with a hypothetical charge separation distance  $r^*$ , defined as

$$E_{\text{int}}(\Delta r = 1.3) = -\frac{1}{4\pi\epsilon_0} \frac{q_e q_c}{r^*} \quad (2)$$

At  $\Delta r = 1.3 \text{ \AA}$ , the value of  $r^*$  is  $6.5 \text{ \AA}$ , which places the hypothetical negative point charge approximately half-way between the  $\text{O}_c$  atom and the phosphorus atom. It may be expected that, in the absence of a counter-ion, the negative

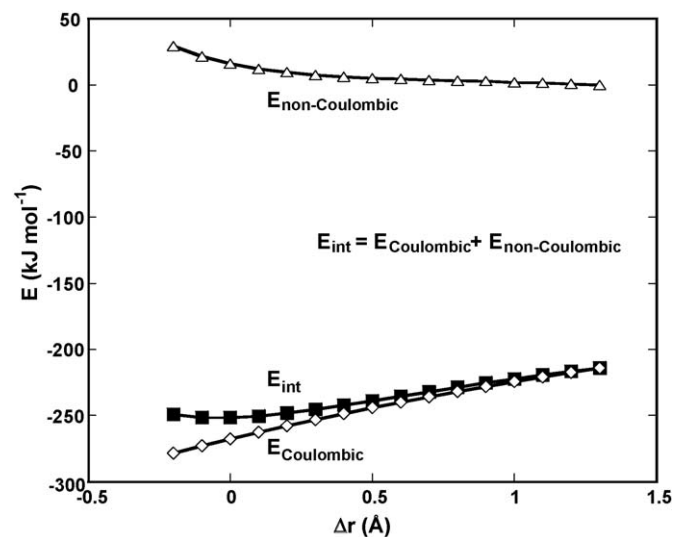


Fig. 5. The interaction energy of a carbenium ion over HPW as a function of the distance displaced from the optimal position. The carbenium-ion was displaced in increments of  $0.1 \text{ \AA}$  along the vector connecting the central P and the  $\text{O}_c$  atom labeled in Fig. 1: (■) The interaction energy as defined in Eq. (1); (◇) the attractive Coulombic contribution to the interaction energy; and (△) the non-Coulombic repulsive interaction energy.

charge in the conjugate base distributes somewhat evenly over the entire Keggin unit. However, at  $\Delta r = 1.3$  Å, the negative charge of the conjugate base is not delocalized evenly over the entire Keggin unit, but is distributed more in the half of the Keggin unit closer to the carbenium ion. Using the difference between the actual displacement,  $\Delta r$ , at each single-point geometry and assuming the charge distribution in the Keggin unit remains constant (reasonable for small displacements), the interaction of the carbenium ion with the catalyst can be approximated as the addition of Coulombic and non-Coulombic terms

$$E_{\text{int}}(\Delta r) = E_{\text{Coulombic}}(\Delta r) - E_{\text{non-Coulombic}}(\Delta r)$$

$$= -\frac{1}{4\pi\epsilon_0} \frac{q_e q_c}{r^* - (1.3 - \Delta r)} + E_{\text{non-Coulombic}}(\Delta r) \quad (3)$$

Fig. 5 illustrates that at larger displacement distances, the total interaction energy is approximated by a purely Coulombic interaction. The non-Coulombic interaction is repulsive, increasing in strength as the carbenium ion is moved closer to the catalyst. The optimal position balances the attractive Coulombic interaction and the repulsive non-Coulombic interaction. The similar slopes for these two interactions taken at the equilibrium position generates a flat PES for small carbenium-ion displacements ( $<0.3$  Å). At the equilibrium position, the attractive Coulombic interaction is  $-267.6$  kJ mol $^{-1}$  and the repulsive interaction is  $+16.1$  kJ mol $^{-1}$ .

As mentioned in Section 1, the transition states for many hydrocarbon conversion processes are carbenium ions. In the next two sections, we describe the results of calculations of the transition states for the elementary reactions of isobutane dehydrogenation and 2-methyl-2-propanol dehydration. The transition states for both of these processes are found to be *t*-butyl carbenium ions.

### 3.3. Isobutane dehydrogenation

Milas and Nascimento have shown that the protolysis of isobutane, activated by donation of a proton to form molecular hydrogen and an adsorbed *t*-butyl intermediate, occurs through a carbenium-ion transition state in HZSM-5 [27,28]. Here we show similar results for the protolysis of isobutane over HPW. These results indicate that the transition state is a carbenium ion, with a tri-coordinate carbon atom, rather than a carbonium ion with a pentacoordinate carbon, as proposed by the Haag-Dessau mechanism [40]. The DFT-calculated interaction energy for the initial approach of isobutane to HPW is thermoneutral. It is well-established, however, that the interaction of alkanes with a zeolite is underpredicted using DFT methods as most gradient-corrected functionals do not accurately determine the weak dispersive forces responsible for the adsorption of the alkane [27]. The same interactions are also likely operative in the adsorption of alkanes to the surface of the Keggin structures described herein. The product of protolysis is an adsorbed *t*-butyl alkoxide (assumed to reside on an O<sub>d</sub> atom) and a hydrogen molecule. The transition state for protolysis, shown in Fig. 6, resembles a *t*-butyl carbenium along with a

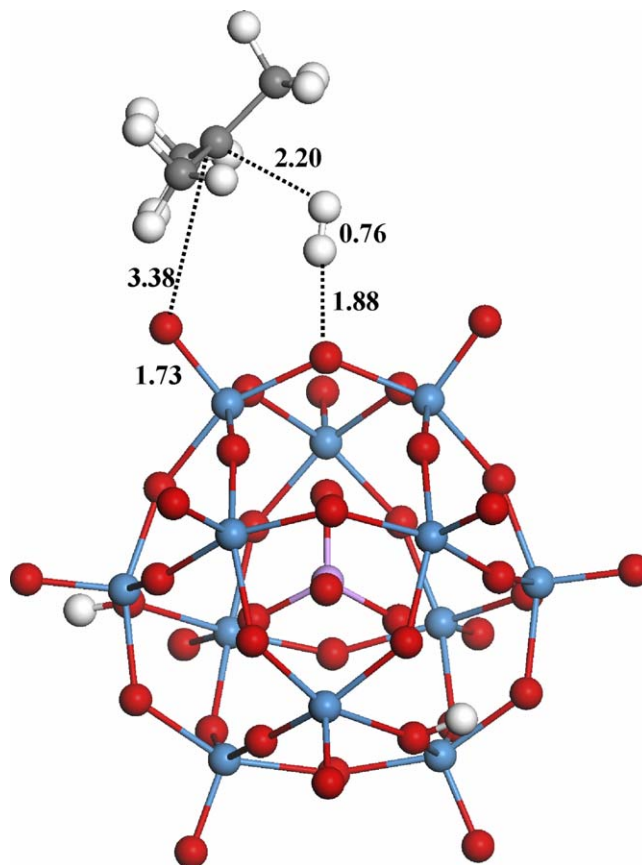


Fig. 6. The transition state for protolysis of isobutane to form an adsorbed *t*-butyl alkoxide and a hydrogen molecule. The activation barrier is 162.8 kJ mol $^{-1}$ . Distances are in Å.

completely formed hydrogen molecule. Additional transition state searches between the initial and *t*-butyl carbenium-ion state indicate that this is the only possible transition state. The energy monotonically increases as the tertiary C–H bond is broken and molecular hydrogen formed. The activation barrier for protolysis is 162.8 kJ mol $^{-1}$ , which is lower than the value reported over HZSM-5, 194 kJ mol $^{-1}$  [28]. The transition state contains a single imaginary frequency of 71i cm $^{-1}$ , and the total number of valence electrons is 24.77, consistent with a *t*-butyl carbenium ion. Removal of the hydrogen molecule, and subsequent optimization, changes the carbenium-ion geometry only slightly, and the interaction of H<sub>2</sub> with HPW and/or the carbenium ion is less than 10 kJ mol $^{-1}$ . The transition state structure with molecular hydrogen removed is 36.1 kJ mol $^{-1}$  higher in energy than structure C of Fig. 2 (the intermediate for *t*-butyl adsorption), as the positively charged carbenium-ion is farther from the Keggin unit.

### 3.4. 2-Methyl-2-propanol dehydration

A 2-methyl-2-propanol (2M2P) molecule initially adsorbs to the HPW Keggin structure by forming a hydrogen bond between the oxygen atom of the alcohol and a proton of the solid acid. Dehydration then proceeds by the donation of the proton to the alcohol to form a water molecule, breaking of the C–O alcohol bond, and adsorption of the *t*-butyl group to the

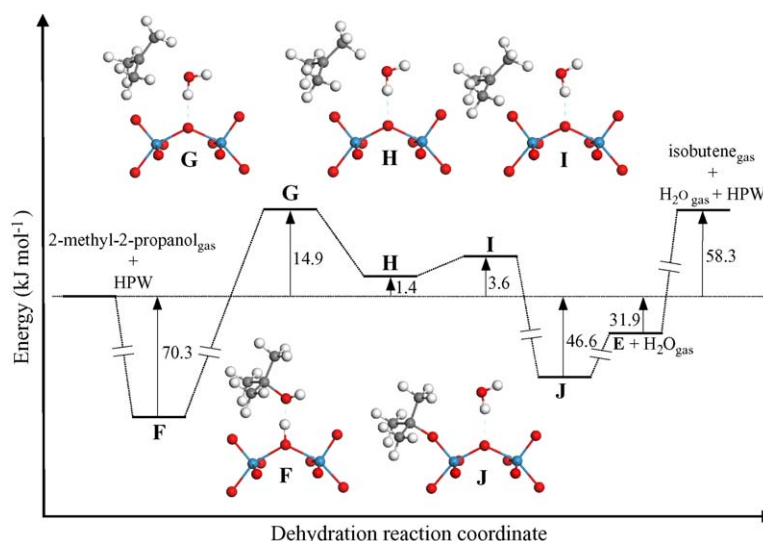


Fig. 7. Reaction energy diagram for the dehydration of 2-methyl-2-propanol over phosphotungstic acid. Interatomic distances within these structures are given in Table 3. Only a portion of the Keggin unit is shown; however, all calculations were performed with the entire Keggin unit.

conjugate base of the acid as an alkoxide [22]. The adsorbed *t*-butyl group can then desorb as isobutene as described above. Over HPW, a meta-stable *t*-butyl carbenium intermediate appears to form along the dehydration reaction path.

The reaction energy diagram for the dehydration of 2M2P is shown in Fig. 7, with interatomic distances and other specifications for each extremum given in Table 3. The initial adsorption of 2M2P to the hydrogen bound state (state F in Fig. 7) is exothermic by  $-70.3 \text{ kJ mol}^{-1}$ . The dehydration of 2M2P is endothermic by  $23.7 \text{ kJ mol}^{-1}$  relative to adsorbed state F, producing a *t*-butyl alkoxide intermediate and a water molecule that is hydrogen bound to the Keggin unit (state J in Fig. 7). The desorption of the water molecule, leaving the *t*-butyl alkoxide, is endothermic by  $14.7 \text{ kJ mol}^{-1}$ . The overall dehydration reaction is completed by the endothermic desorption of the *t*-butyl fragment as isobutene, thus regenerating the active surface site. The overall calculated dehydration reaction energy (alcohol to alkene plus water) is  $+58.3 \text{ kJ mol}^{-1}$ .

A single NEB-CI calculation between states F and J produces a structure that, following optimization, has all real frequencies and is therefore a meta-stable intermediate (H). The C–C bond distances (1.42–1.47 Å), planarity of the tertiary

carbon, and the charge distribution (24.77 valence electrons for the alkyl fragment) are consistent with a carbenium ion like *t*-butyl fragment. There is little interaction of the *t*-butyl fragment with the water molecule, as removal of the water molecule and re-optimization does not perturb the *t*-butyl geometry. The desorption of the water molecule from state H (leaving the adsorbed carbenium ion) is endothermic by  $66.8 \text{ kJ mol}^{-1}$ , as a strong hydrogen bond is formed between the water molecule and the negatively charged Keggin unit. Structure H without the water molecule can be directly compared with the carbenium-ion intermediate for isobutene adsorption (structure C in Fig. 2) as they both then represent *t*-butyl carbenium ions over the HPW surface. Structure H without the water molecule is less stable than structure C because the *t*-butyl species is located farther from the Keggin unit.

Two NEB-CI transition state searches were performed between each of the equilibrium states (F, J) and the carbenium-ion intermediate (H). The transition state located between the hydrogen bound state (F) and the intermediate (H) is labeled state G in Fig. 7. The activation barrier from the hydrogen bound state (F) is  $85.2 \text{ kJ mol}^{-1}$ . This transition state shows three imaginary frequencies:  $88i$ ,  $107i$ , and  $221i \text{ cm}^{-1}$ . The first of these vibrational modes appears as the reaction

Table 3

The relative energies, imaginary frequencies, and interatomic distances of the equilibrium and transition states for 2-methyl-2-propanol dehydration over phosphotungstic acid

State <sup>a</sup>	RE <sup>b</sup> (kJ mol <sup>-1</sup> )	Imag freq. (cm <sup>-1</sup> )	No. valence electrons <sup>c</sup>	O <sub>c</sub> –H <sup>+</sup> (Å)	H <sup>+</sup> –O <sub>alc</sub> (Å)	C <sup>2</sup> –O <sub>alc</sub> (Å)	C <sup>2</sup> –O <sub>d</sub> (Å)	W–O <sub>d</sub> (Å)
F	–70.3	None	25.02	1.09	1.39	1.51	3.58	1.71
G	14.9	88 <i>i</i> , 107 <i>i</i> , 221 <i>i</i>	24.79	1.79	0.99	2.93	3.43	1.73
H	1.4	None	24.77	1.85	0.99	3.41	3.09	1.73
I	3.6	113 <i>i</i>	24.78	1.83	0.99	3.73	2.39	1.74
J	–46.6	None	24.98	2.01	0.98	4.24	1.50	1.80

<sup>a</sup> The states for adsorption are illustrated in Fig. 7, and discussed in the text.

<sup>b</sup> Energy given relative to separated 2-methyl-2-propanol and phosphotungstic acid.

<sup>c</sup> Number of valence electrons included those allocated to the *t*-butyl fragment of 2-methyl-2-propanol (four C atoms and nine H atoms).

coordinate, with the C<sup>2</sup>–O alcohol bond stretching and rehybridization of C<sup>2</sup> from sp<sup>3</sup> to sp<sup>2</sup>. The other two modes are mainly methyl rotations, with minor coupling to the reaction mode. Displacement along these modes followed by optimization converges to a minimum along the reaction coordinate. The optimization of the methyl rotations does not typically change the total energy by more than a few kJ mol<sup>−1</sup>. The structure and charge of the *t*-butyl group in state **G** is consistent with a carbenium ion.

A second transition state was located between states **H** and **J**, and is labeled state **I**. In state **I**, the *t*-butyl carbenium ion has moved closer to the Keggin unit, seen by a decrease in the C–O<sub>d</sub> distance, in order to facilitate formation of the alkoxide bond. State **I** is only 2.4 kJ mol<sup>−1</sup> less stable than state **H** and has a single imaginary frequency of 113i cm<sup>−1</sup>, indicating that formation of the alkoxide state from the *t*-butyl carbenium ion occurs over a small barrier on a flat PES. The similarity of the reaction coordinate for dehydration of 2-methyl-2-propanol and the adsorption of isobutene confirms the importance of carbenium ions as transition states and intermediates for hydrocarbon conversion processes over phosphotungstic acid.

#### 4. Conclusions

Tertiary carbenium ions represent both transition states and high-energy meta-stable intermediates for various hydrocarbon conversion processes over phosphotungstic acid. The potential energy surface for conversion of the *t*-butyl carbenium ion to a  $\pi$ -bound state or an alkoxide is relatively flat, in which the majority of the interaction of the alkyl species with the catalyst surface is Coulombic in nature. The reaction coordinate for the adsorption of isobutene to phosphotungstic acid includes a carbenium-ion intermediate. Proton donation and alkoxide formation occur in a step-wise fashion over two distinct transition states. Along with isobutene adsorption, *t*-butyl carbenium ions represent transition states for isobutane dehydrogenation and 2-methyl-2-propanol dehydration, emphasizing the importance of these species for hydrocarbon transformations over solid acid catalysts.

#### Acknowledgements

This work was funded by the National Science Foundation (CTS-0124333). This research was performed in part using the Molecular Science Computing Facility (MSCF) in the William R. Wiley Environmental Molecular Sciences Laboratory, a national scientific user facility sponsored by the U.S. Department of Energy's Office of Biological and Environmental Research and located at the Pacific Northwest National Laboratory. Pacific Northwest is operated for the Department of Energy by Battelle.

#### References

- [1] J.F. Haw, B.R. Richardson, I.S. Oshiro, N.D. Lazo, J.A.J. Speed, *Am. Chem. Soc.* 111 (1989) 2052–2058.
- [2] E.G. Derouane, H. He, S.B. Derouane Abd-Hamid, I.I. Ivanova, *Catal. Lett.* 58 (1999) 1–19.
- [3] A. Corma, A. Martinez, *Catal. Rev. Sci. Eng.* 35 (1993) 483–570.
- [4] A. Feller, I. Zuazo, A. Guzman, J.O. Barth, J.A. Lercher, *J. Catal.* 216 (2003) 313–323.
- [5] J. Weitkamp, Y. Traa, Alkylation of isobutane with alkenes on solid catalysts, in: G. Ertl, H. Knozinger, J. Weitkamp (Eds.), *Handbook of Heterogeneous Catalysis*, vol. 4, VCH Verlagsgesellschaft, Weinham, 1997, pp. 2039–2069.
- [6] A. Feller, A. Guzman, I. Zuazo, J.A. Lercher, *J. Catal.* 224 (2004) 80–93.
- [7] M.T. Pope, *Heteropoly and Isopoly Oxometalates*, vol. 8, Springer-Verlag, New York, 1983, p. 180.
- [8] T. Okuhara, N. Mizuno, M. Misono, *Adv. Catal.* 41 (1996) 113–252.
- [9] I.V. Kozhevnikov, *Russ. Chem. Rev.* 56 (1987) 811–825.
- [10] B.B. Bardin, S.V. Bordawekar, M. Neurock, R.J. Davis, *J. Phys. Chem. B* 102 (1998) 10817–10825.
- [11] K.A. Campbell, M.J. Janik, M. Neurock, R.J. Davis, *Langmuir* 21 (2004) 4738–4745.
- [12] V.B. Kazansky, I.N. Senchenya, *J. Mol. Catal.* 74 (1992) 257–266.
- [13] P.E. Sinclair, A. de Vries, P. Sherwood, C.R.A. Catlow, R.A. van Santen, *J. Chem. Soc., Faraday Trans. 94* (1998) 3401–3408.
- [14] A. Bhan, Y.V. Joshi, W.N. Delgass, K.T. Thomson, *J. Phys. Chem. B* 107 (2003) 10476–10487.
- [15] X. Rozanska, T. Demuth, F. Hutschka, J. Hafner, R.A. van Santen, *J. Phys. Chem. B* 106 (2002) 3248–3254.
- [16] X. Rozanska, R.A. van Santen, T. Demuth, F. Hutschka, J. Hafner, *J. Phys. Chem. B* 107 (2003) 1309–1315.
- [17] P. Viruela-Martin, C.M. Zicovich-Wilson, A. Corma, *J. Phys. Chem.* 97 (1993) 13713–13719.
- [18] V.B. Kazansky, M.V. Frash, R.A. van Santen, *Appl. Catal. A* 146 (1996) 225–247.
- [19] M. Boronat, P.M. Viruela, A. Corma, *J. Am. Chem. Soc.* 126 (2004) 3300–3309.
- [20] L. Benco, J. Hafner, F. Hutschka, H. Toulhoat, *J. Phys. Chem. B* 107 (2003) 9756–9762.
- [21] A.M. Rigby, G.J. Kramer, R.A. van Santen, *J. Catal.* 171 (1997) 1–10.
- [22] M.T. Aronson, R.J. Gorte, W.E. Farneth, D. White, *J. Am. Chem. Soc.* 111 (1989) 840–846.
- [23] C.M. Zicovich-Wilson, P. Viruela, A. Corma, *J. Phys. Chem.* 99 (1995) 13224–13231.
- [24] M. Guisnet, N.S. Gnep, *Appl. Catal. A* 146 (1996) 33–64.
- [25] V.B. Kazansky, *Catal. Today* 51 (1999) 419–434.
- [26] S.R. Blaszkowski, A.P.J. Jansen, M.A.C. Nascimento, R.A. van Santen, *J. Phys. Chem.* 98 (1994) 12938–12944.
- [27] I. Milas, M.A.C. Nascimento, *Chem. Phys. Lett.* 338 (2001) 67–73.
- [28] I. Milas, M.A.C. Nascimento, *Chem. Phys. Lett.* 373 (2003) 379–384.
- [29] M.A. Natal-Santiago, R. Alcalá, J.A. Dumesic, *J. Catal.* 181 (1999) 124–144.
- [30] M.V. Frash, V.B. Kazansky, A.M. Rigby, R.A. van Santen, *J. Phys. Chem. B* 102 (1998) 2232–2238.
- [31] G. Kresse, J. Hafner, *Phys. Rev. B* 47 (1993) 558–561.
- [32] G. Kresse, J. Furthmüller, *Comput. Mater. Sci.* 6 (1996) 15–50.
- [33] G. Kresse, J. Furthmüller, *Phys. Rev. B* 54 (1996) 11169–11186.
- [34] D. Vanderbilt, *Phys. Rev. B* 41 (1990) 7892–7895.
- [35] J.P. Perdew, J.A. Chevary, S.H. Vosko, K.A. Jackson, M.R. Pederson, D.J. Singh, C. Fiolhais, *Phys. Rev. B* 46 (1992) 6671–7895.
- [36] M.J. Janik, K.A. Campbell, B.B. Bardin, R.J. Davis, M. Neurock, *Appl. Catal. A* 256 (2003) 51–68.
- [37] G. Mills, H. Jonsson, G.K. Schenter, *Surf. Sci.* 324 (1995) 305–337.
- [38] G. Henkelman, H. Jonsson, *J. Chem. Phys.* 113 (2000) 9978–9985.
- [39] G. Henkelman, B.P. Uberuaga, H. Jonsson, *J. Chem. Phys.* 113 (2000) 9901–9904.
- [40] S. Kotrel, H. Knozinger, B.C. Gates, *Micro. Meso. Mater.* 35–36 (2000) 11–20.